

Synchronized dual-wavelength mode-locked laser in normal dispersion regime

Yangrui Shi(史洋瑞), Haojing Zhang(张皓景), Yuxuan Ren(任俞宣), Junsong Peng(彭俊松), and Heping Zeng(曾和平)

Citation: Chin. Phys. B, 2025, 34 (**9**): 094207. DOI: 10.1088/1674-1056/add4fe
http://cpb.iphy.ac.cn; http://iopscience.iop.org/cpb

What follows is a list of articles you may be interested in

Generation ofWatt-level Kerr-lens mode-locked Yb:CYA laser at 1-GHz repetition rate

Guodong Zhao(赵国栋), Junyi Ma(马骏逸), Hainian Han(韩海年), Zhaohua Wang(王兆华), and Zhiyi Wei(魏志义)

Chin. Phys. B, 2025, 34 (**8**): 084204. DOI: 10.1088/1674-1056/adcf8b

TaS_2-based saturable absorbers for *Q*-switched fiber laser applications

Qinghua Wang(汪情华), Hao Sun(孙昊), Chenhao Lu(鲁晨浩), Huiran Yang(杨慧苒), and Lu Li(李璐)

Chin. Phys. B, 2025, 34 (**7**): 074209. DOI: 10.1088/1674-1056/addcd7

Multi-wavelength and transversely mode-switchable fiber laser based on ring-core fiber Bragg grating

Ya-Jun Jiang(姜亚军), Yu-Hui Su(苏宇辉), Jia-Xin Gao(高嘉欣), Feng Zhou(周峰), Li-Qin Cheng(程丽琴), Kang-Wei Pan(潘康伟), Bin-Chuan Sun(孙镔传), Li Shen(申力), De-Xing Yang(杨德兴), and Jian-Lin Zhao(赵建林)

Chin. Phys. B, 2025, 34 (**6**): 064203. DOI: 10.1088/1674-1056/adc663

High-efficiency Yb^{3+}-doped fiber laser with highly optical nonlinear Bi_4Br_4-based saturable absorber

Mengyuan Liu(刘梦媛), Yechao Han(韩烨超), Qi Liu(刘齐), Hao Teng(滕浩), Xiwei Huang(黄玺玮), Xiaowei Xing(邢笑伟), Xiangyu Qiao(乔向宇), Guojing Hu(胡国静), Xiao Lin(林晓), Haitao Yang(杨海涛), Zhiyi Wei(魏志义), and Wenjun Liu(刘文军)

Chin. Phys. B, 2025, 34 (**6**): 064202. DOI: 10.1088/1674-1056/adc664

Pure-quartic soliton molecules in normal fourth-order dispersion regimes based on spectral filtering effect

Han-Yang Shen(申翰阳), Rui-Bo Lan(蓝睿博), Hong-Bin Hu(胡洪彬), Yang Li(李阳), Rui Zhou(周瑞), and Zu-Xing Zhang(张祖兴)

Chin. Phys. B, 2025, 34 (**3**): 034203. DOI: 10.1088/1674-1056/ada43c

---

Synchronized dual-wavelength mode-locked laser in normal dispersion regime

Yangrui Shi(史洋瑞)[1], Haojing Zhang(张皓景)[1,2], Yuxuan Ren(任俞宣)[1], Junsong Peng(彭俊松)[1,2,†], and Heping Zeng(曾和平)[1,2,3]

[1] *State Key Laboratory of Precision Spectroscopy, and Hainan Institute, East China Normal University, Shanghai* 200062, *China*
[2] *Chongqing Key Laboratory of Precision Optics, Chongqing Institute of East China Normal University, Chongqing* 401120, *China*
[3] *Chongqing Institute for Brain and Intelligence, Guangyang Bay Laboratory, Chongqing* 400064, *China*

(Received 28 February 2025; revised manuscript received 17 April 2025; accepted manuscript online 7 May 2025)

Synchronized dual-wavelength mode-locked laser is investigated numerically and experimentally in the normal dispersion regime. A programmable optical processor is introduced to shape the spectral profile and adjust the net dispersion, which is demonstrated be a convenient and reliable approach to generate dual-color solitons. The time-stretch dispersive Fourier transform and frequency-resolved optical grating techniques are utilized to measure the spectral and temporal characteristics of dual-color solitons, respectively. The numerical results are consistent with experimental results. This work may facilitate the development of filter-based mode-locked laser and the understanding of multi-wavelength soliton dynamics.

Keywords: fiber laser, mode locking, dual-wavelength

PACS: 42.55.Wd, 42.65.–k, 42.65.Re, 42.65.Tg

DOI: 10.1088/1674-1056/add4fe **CSTR:** 32038.14.CPB.add4fe

1. Introduction

Solitons are localized waves propagating without spreading under diffraction/dispersive mediums. They can be readily generated in a mode-locked laser resulting from the balance between dispersion, nonlinearity, gain and dissipation.[1–4] Through the synchronization of solitons at different wavelengths, multi-wavelength laser can be obtained.[5–8] Dual-wavelength light sources have a wide range of applications ranging from microwave and terahertz signal generation,[9–15] to Raman spectroscopy imaging,[16,17] and nonlinear frequency conversion.[18,19] Furthermore, the dual-color solitons obtained by dual-wavelength mode locking are analogous to chemical molecular structures,[20] holding significant implications for interdisciplinary fundamental research.[21,22] Dual-color solitons also offer a novel pathway for synthesizing single-cycle waveforms in nanophotonics.[23]

Mode-locked fiber lasers in different dispersion regions have different features.[3] Synchronized dual-wavelength mode-locking was previously mainly studied in negative dispersion regions.[5–7] In this dispersion regime, the interference between dispersive waves and solitons can result in the generation of Kelly sidebands, which causes instabilities in the laser.[24] Kelly sidebands can be avoided by operating the fiber laser in the normal dispersion regime. Though multi-wavelength mode locking was extensively studied in the normal dispersion regime,[25] due to dispersion, the different frequency components are not synchronized, leading to periodic walk-off of the pulses in the lasers.[26–28]

In recent years, spectral phase shaping technology has demonstrated remarkable advantages in dispersion compensation for mode-locked fiber lasers. Its core principle lies in the active manipulation of the spectral phase of pulses via programmable optical processor, as opposed to relying on traditional passive compensation schemes using dispersion-managed fibers.[29–31] This technology has now been successfully applied to diverse scenarios, including multi-wavelength synchronization,[5,32] soliton molecule manipulation,[33] and the excitation of novel soliton states.[6,34–37]

Here, we present a convenient and reliable method for generating synchronized dual-wavelength mode-locked fiber laser in the normal dispersion regime, using a programmable optical processor (Finisar, Waveshaper 1000A). The dual-color solitons can be generated with a dual-humped filter. The phase and amplitude of each passband of the filter can be independently controlled, realizing in dispersion management and transmission control of the filter simultaneously. A frequency-resolved optical gating (FROG) is utilized to measure the temporal profile of the dual-color soliton, confirming the interference-like patterns on the temporal waveforms. The stability of output pulses is verified by time-stretch dispersive Fourier transform (TS-DFT) technique.[38] and radio frequency (RF) analyzer. The simulation results based on the generalized nonlinear Schrödinger equation (NLSE) are in good agreement with the experimental results.

†Corresponding author. E-mail: jspeng@lps.ecnu.edu.cn

© 2025 Chinese Physical Society and IOP Publishing Ltd. All rights, including for text and data mining, AI training, and similar technologies, are reserved.

2. Experimental setup

The laser setup is shown in Fig. 1, which is a typical scheme for passively mode-locked fiber laser. A 980-nm laser diode is used to pump the erbium-doped fiber (EDF) through a 980-nm/1550-nm wavelength-division-multiplexer. The EDF (OFS-EDF80) has 1.3-m-long with second-order group velocity dispersion (GVD) of 62.5 ps^2/km, and the rest of the cavity consists of standard single-mode fiber with GVD of -22.8 ps^2/km. The laser is mode-locked by nonlinear polarization rotation. The polarization controller initializes mode-locking operation by controlling the polarization state, and the isolator ensures unidirectional operation of the ring cavity. Waveshaper is a programmable optical processor utilizing a high-resolution solid-state liquid crystal on silicon array. It disperses input light by wavelength via a grating, independently adjusts each component's amplitude and phase, then recombines them to generate tailored output signals, enabling precise spectral filtering and dispersion management. The optical coupler extracts 10% energy for measurement. Though the estimated net GVD of the ring cavity from the fibers is -0.32 ps^2, it can be compensated to achieve normal dispersion with the waveshaper.

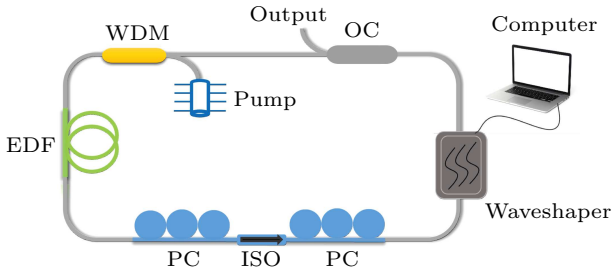


Fig. 1. Experimental setup of the dual-wavelength mode-locked laser. WDM: wavelength-division multiplexer; EDF: erbium-doped fiber; PC: polarization controller; ISO: isolator; OC: optical coupler.

3. Experimental results

The net dispersion in the cavity can be controlled by adjusting the curvature of the parabolic spectral phase profile in the waveshaper. The positive dispersion of the cavity increases with the convexity of the phase curve. The spectral profile can be precisely manipulated by setting attenuation on the different positions on spectra in frequency domain. For the waveshaper, we have configured a filtering function featuring double rectangular peaks. To ensure the cavity operates entirely within the positive dispersion regime, we incorporated a net dispersion of 0.65 ps^2, achieving a net cavity dispersion of 0.33 ps^2 (contrasting with the original net dispersion of -0.32 ps^2). The transmission of the waveshaper is described by the following equation:[39]

$$H(\omega) = R(\omega)G(\omega), \tag{1}$$

where $R(\omega)$ denotes the Fourier transform of a certain objective function, and the spectral phase adds a specific amount of GVD to the cavity. Here, we set the spectral profile as

$$R(\omega) = \begin{cases} 1, & \omega_1 \le \omega \le \omega_2 \ \text{ or } \ \omega_3 \le \omega \le \omega_4, \\ 0, & \text{otherwise}, \end{cases} \tag{2}$$

where ω_1, ω_2, ω_3, ω_4 determines the bandwidths of the rectangular filter. $G(\omega)$ represents the parabolic phase function, whose specific form is

$$G(\omega) = \exp\left[\mathrm{i}\beta_{2,\mathrm{acc}}\omega^2/2\right]. \tag{3}$$

By varying the parabolic phase function of $G(\omega)$, we can control the net dispersion of the cavity. The second-order dispersion can be added through the term $\beta_{2,\mathrm{acc}}$ (in unit ps^2). The curve of $H(\omega)$ is shown in Fig. 2 where the black solid line represents $R(\omega)$, and the red dashed line represents $G(\omega)$. The curve is used for both the experiment and simulation.

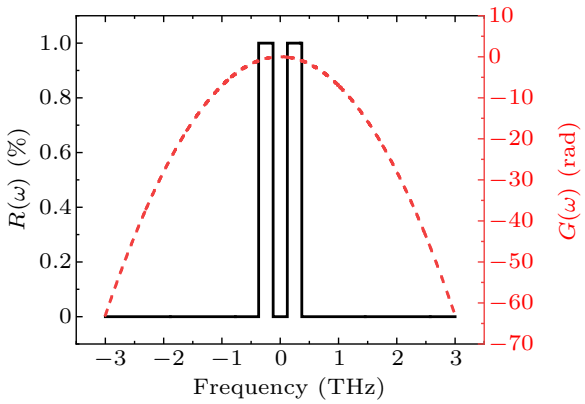


Fig. 2. The filter function diagram of the waveshaper for both the experiment and simulation.

In the experiment, dual-wavelength mode locking is achieved by adjusting the PC. The stable output of dual-color solitons can be achieved under a pump power of 38 mW. Figure 3(a) shows the dual-peak spectral profile measured by an optical spectrum analyzer. The optical spectrum of the pulses is determined by the waveshaper, exhibiting central wavelengths at 1555 nm and 1559 nm and a bandwidth of 2 nm of each wavelength band. The different gain coefficients at the two wavelengths lead to different intensities between them. The real-time evolution of the optical spectrums is also measured as seen in Fig. 3(b), indicating the stability of such a mode-locked state. The dual-wavelength optical spectrum exhibits only a single repetition rate as measured by a radio frequency analyzer with a high resolution of 1 Hz (Fig. 3(c)), indicating that the two wavelengths are synchronized. The fundamental repetition rate of 10.826 MHz matches the cavity length, with a signal-to-noise ratio of 50 dB, confirming stable mode-locking.

The temporal intensity measurement using a photodetector shows only a single pulse, and cannot unveil the detailed interference-like patterns of the pulse under dual-wavelength

mode locking. To further reveal the detailed pulse profiles, an FROG is employed, which can measure the temporal profiles of ultrashort pulses with a high resolution (~ 30 fs).[40,41] Figure 3(d) shows an excellent agreement between FROG-retrieved and measured spectrograms, validating the reliability of the time domain measurement results. The detailed waveform of the pulse is shown in Fig. 3(e), showing an interference-like structure with a period of 1.8 ps. Such a period is determined by the separation between the two wavelengths (4 nm), as a result of Fourier transformation.

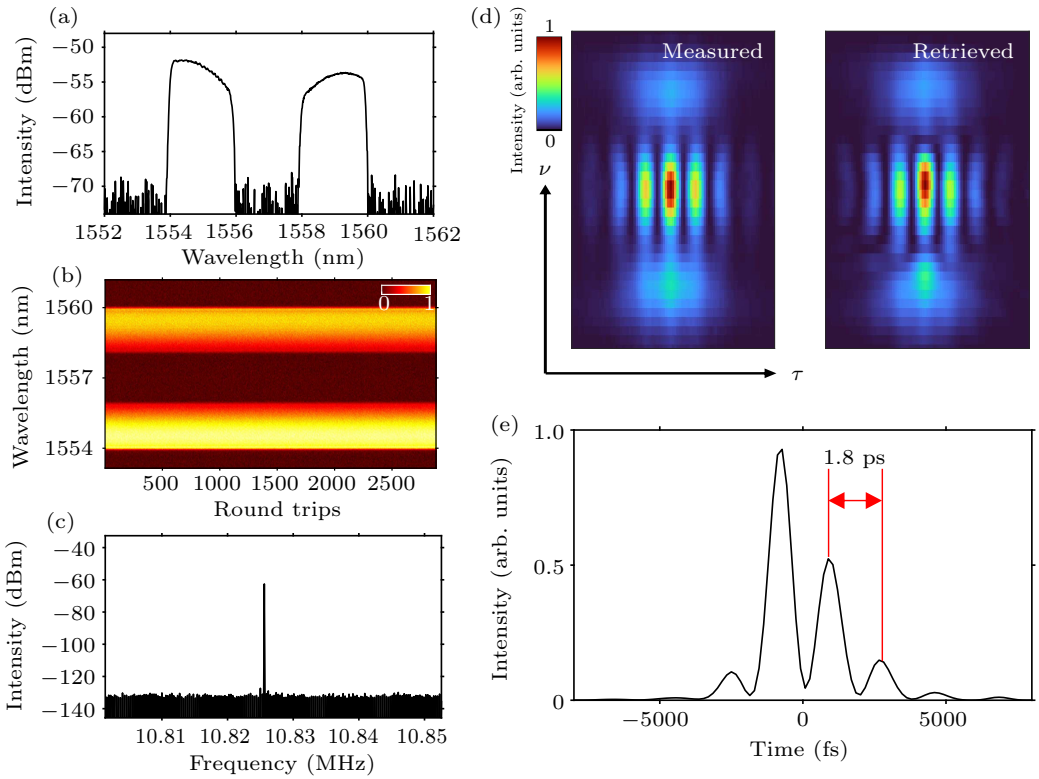


Fig. 3. The output pulse properties of the dual-wavelength mode-locked fiber laser in the experiment: (a) Output spectrum, (b) the real-time spectral evolution measured using DFT, (c) RF spectrum, (d) measured (left panel) and retrieved (right panel) FROG spectrograms, (e) the retrieved temporal profile.

4. Numerical simulations

To verify the experimental results, we performed numerical simulations based on the generalized NLSE[42]

$$\psi_z = -\frac{\mathrm{i}\beta_2}{2}\psi_{tt} + \mathrm{i}\gamma|\psi|^2\psi + \frac{g}{2}\left(\psi + \frac{1}{\Omega^2}\psi_{tt}\right), \tag{4}$$

where $\psi = \psi(z,t)$ represents the slowly varying electric field, and z is the moving coordinate. The coefficients β_2 and γ denote the group velocity dispersion and Kerr nonlinearity coefficients, respectively. In this simulation, we set fixed values of $\beta_2 = 62.5$ ps^2/km and -22.5 ps^2/km for EDF and SMF, respectively. For γ, we take 8 W^{-1}·km^{-1} and 1.5 W^{-1}·km^{-1} for EDF and SMF, respectively. The dissipative terms account for linear gain and approximate the gain profile using a parabolic approximation with full width at half-maximum (FWHM) bandwidth Ω of 40 nm. The gain is saturated according to the function

$$g(z) = g_0/[1 + E(z)/E_{\mathrm{sat}}], \tag{5}$$

where $g_0 = 1500$ km^{-1} represents the small-signal gain of EDF, $E(z) = \int |\psi(z,t)|^2 \mathrm{d}t$ represents the pulse energy, and $E_{\mathrm{sat}} = 100$ pJ is the gain saturation energy determined by the pump power. For SMF, g is set to be zero. We employed nonlinear polarization rotation technology in our experimental setup. Our model takes into account a generic saturated absorption function, providing an instantaneous and monotonically increasing nonlinear transfer function for pulse power:

$$T = \sqrt{1 - q_0 - q_{\mathrm{m}}/[1 + P(t)/P_{\mathrm{sat}}]}, \tag{6}$$

where q_0 represents the unsaturated loss, q_{m} indicates the saturable loss (modulation depth), $P(t) = |\psi(z,t)|^2$ represents the instantaneous power of the pulse, and P_{sat} represents the saturation power. q_0, q_{m}, and P_{sat} are set to be 0.3, 0.7, and 10 W in the simulations, respectively. The filter function is the same as that used in the experiments, as shown in Fig. 1.

Figure 4(a) shows the pulse spectrum of dual-wavelength mode locking in the simulations. The central wavelengths of the dual-wavelength spectrum are 1555 nm and 1559 nm, respectively. The dual-color solitons also show modulation in the time domain, with a period of 2 ps in good agreement with the experimental value (1.8 ps).

Our simulation also reveals the formation dynamics of the dual-wavelength solitons. As shown in Fig. 5(a), although the

initial condition is a Gaussian pulse, under the influence of dual-humped spectral filtering, dual-color solitons with modulated temporal intensities are generated finally. Simultaneously, the initial optical spectrum with a central wavelength of 1560 nm evolves into a dual-peak profile with central wavelengths of 1555 nm and 1559 nm determined by the filter, as shown in Fig. 5(b). However, since mode locking at the normal dispersion regime is difficult to self-start, the corresponding experiments cannot be recorded.

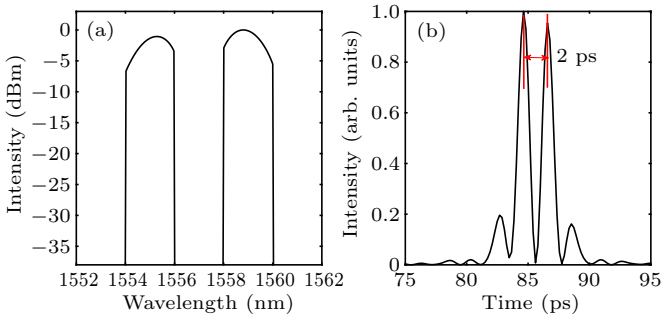


Fig. 4. Simulation results of dual-wavelength mode-locked solitons: (a) optical spectrum, (b) the temporal profile of the pulses.

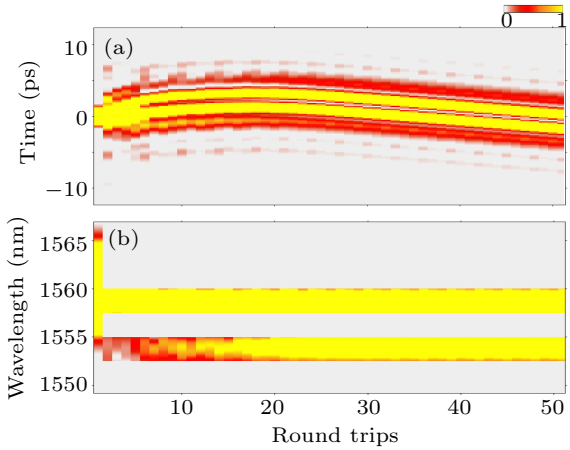


Fig. 5. Simulation results of the dual-wavelength mode-locking startup process. (a) The temporal waveform evolution and (b) the spectral evolution.

5. Conclusion

We realized a synchronized dual-wavelength mode-locked fiber laser in the normal dispersion regime by virtue of employing a waveshaper in the cavity. The waveshaper allowing independent controlling of the phase and transmission of each passband of the filter, plays a key role in the laser operation. Experimental results are confirmed with simulations. Our work may contribute to the understanding of multi-wavelength soliton dynamics and bring new insights into the design of ultrafast lasers. Furthermore, the work also stimulates the study of the multiple pulse generation in the laser. It is of great interesting to see how these solitons with modulated temporal profiles interact with each other.

Acknowledgements

Project supported by the Innovation Program for Quantum Science and Technology (Grant No. 2023ZD0301000), the National Natural Science Foundation of China (Grant Nos. 12434018, 62475073, 1243000542, 11621404, 11561121003, 11727812, 61775059, 12074122, 62405090, 62035005, and 11704123), the Natural Science Foundation of Shanghai (Grant No. 23ZR1419000), and China Postdoctoral Science Foundation (Grant Nos. 2023M741188 and 2024T170275).

References

[1] Grelu P and Akhmediev N 2012 *Nat. Photon.* **6** 84
[2] Song Y, Shi X, Wu C, Tang D and Zhang H 2019 *Appl. Phys. Rev.* **6** 021313
[3] Kim J and Song Y 2016 *Advances in Optics and Photonics* **8** 465
[4] Han Y, Guo Y, Gao B, Ma C, Zhang R and Zhang H 2020 *Progress in Quantum Electronics* **71** 100264
[5] Mao D, Wang H, Zhang H, Zeng C, Du Y, He Z, Sun Z and Zhao J 2021 *Nat. Commun.* **12** 6712
[6] Zhang H, Mao D, Du Y, Zeng C, Sun Z and Zhao J 2023 *Commun. Phys.* **6** 191
[7] Gao Q, Zhang H, Du Y, Zeng C, Mao D, Grelu P and Zhao J 2025 *Laser & Photonics Reviews* **19** 2400494
[8] Cui Y, Zhang Y, Huang L, Zhang A, Liu Z, Kuang C, Tao C, Chen D, Liu X and Malomed B A 2023 *Phys. Rev. Lett.* **130** 153801
[9] Mo S, Feng Z, Xu S, Zhang W, Chen D, Yang T, Yang C, Li C and Yang Z 2013 *Laser Phys. Lett.* **10** 125107
[10] Ahmad H, Muhammad F D, Pua C H and Thambiratnam K 2014 *IEEE J. Select. Top. Quantum Electron.* **20** 166
[11] Luo Z C, Luo A P and Xu W C 2011 *Applied Optics* **50** 2831
[12] Town G E, Chen L and Smith P W E 2000 *IEEE Photon. Technol. Lett.* **12** 1459
[13] Liu X, Han D, Sun Z, Zeng C, Lu H, Mao D, Cui Y and Wang F 2013 *Sci. Rep.* **3** 2718
[14] Jain A, Chandra N, Anchal A and Kumar K P 2016 *Optics & Laser Technology* **83** 189
[15] Hu G, Mizuguchi T, Zhao X, Minamikawa T, Mizuno T, Yang Y, Li C, Bai M, Zheng Z and Yasui T 2017 *Sci. Rep.* **7** 42082
[16] Ideguchi T, Holzner S, Bernhardt B, Guelachvili G, Picqué N and Hänsch T W 2013 *Nature* **502** 355
[17] Freudiger C W, Yang W, Holtom G R, Peyghambarian N, Xie X S and Kieu K Q 2014 *Nat. Photon.* **8** 153
[18] Zhang F, Gaafar M, Möller C, Stolz W, Koch M and Rahimi-Iman A 2016 *IEEE Photon. Technol. Lett.* **28** 927
[19] Shang Y, Wang P, Li X, Shen M and Xu X 2016 *Optik* **127** 11871
[20] Cui Y, Yao X, Hao X, Yang Q, Chen D, Zhang Y, Liu X, Sun Z and Malomed B A 2024 *Laser & Photon. Rev.* **18** 2300471
[21] Stegeman G I and Segev M 1999 *Science* **286** 1518
[22] He W, Pang M, Yeh D H, Huang J, Menyuk C R and Russell P S J 2019 *Nat. Commun.* **10** 5756
[23] Gray R, Sekine R, Shen M, Zacharias T, Williams J, Zhou S, Chawlani R, Ledezma L, Englebert N and Marandi A 2025 arXiv: 2501.15381 [physics.optics]
[24] Kelly S M J 1992 *Electron. Lett.* **28** 806
[25] Zhang H, Tang D Y, Wu X and Zhao L M 2009 *Opt. Express* **17** 12692
[26] Yang X, Tao J, Lv C, Fu C, Lu B and Bai J 2023 *Opt Express* **31** 37537
[27] Tao J, Fang Y, Song Y, Song P, Hou L, Lu B, Lin Q and Bai J 2022 *Opt. Express* **30** 17465
[28] Guo Z, Liu T, Peng J, Zhu Y, Huang K and Zeng H 2021 *Journal of Lightwave Technology* **39** 3575
[29] Weiner A M 2011 *Opt. Commun.* **284** 3669
[30] Roelens M A F, Frisken S, Bolger J A, Abakoumov D, Baxter G, Poole S and Eggleton B J 2008 *Journal of Lightwave Technology* **26** 73
[31] Peng J and Boscolo S 2016 *Sci. Rep.* **6** 25995
[32] Liu T, Yan M, Guo Z and Zeng H 2022 *Results in Physics* **36** 105464
[33] Zhang Z X, Luo M, Liu J H, Yang Y T, Li T J, Liu M, Luo A P, Xu W C and Luo Z C 2024 *Nat. Commun.* **15** 6148

[34] Han Y, Gao B, Wen H, Ma C, Huo J, Li Y, Zhou L, Li Q, Wu G and Liu L 2024 *Light: Science & Applications* **13** 101
[35] Xue X, Grelu P, Yang B, Wang M, Li S, Zheng X and Zhou B 2023 *Light: Science & Applications* **12** 19
[36] Schröder J, Coen S, Sylvestre T and Eggleton B 2010 *Opt. Express* **18** 22715
[37] Runge A F J, Hudson D D, Tam K K K, de Sterke C M and Blanco-Redondo A 2020 *Nat. Photon.* **14** 492
[38] Goda K and Jalali B 2013 *Nat. Photon.* **7** 102
[39] Boscolo S, Finot C, Karakuzu H and Petropoulos P 2014 *Opt. Lett.* **39** 438
[40] Trebino R and SpringerLink 2000 *Frequency-Resolved Optical Gating: The Measurement of Ultrashort Laser Pulses* (Boston, MA: Springer US)
[41] Keusters D, Tan H S, O'Shea P, Zeek E, Trebino R and Warren W 2003 *J. Opt. Soc. Am. B* **20** 2226
[42] Haus H A 2000 *IEEE J. Select. Top. Quantum Electron.* **6** 1173